A Simple Numerical Model of Thermals and Cumulus Convection

D. Heimann

DFVLR - Oberpfaffenhofen, F.R. Germany

Presented at the XIX. OSTIV Congress, Rieti (Italy), 1985

1. Introduction

Up to now the preparation of weather forecasts for glider flights is mainly based on conventional methods using thermodynamic diagrams and graphical constructions (see for example WMO, 1978). The availability of low-cost personal computers (PC) now opens the possibility of introducing numerical methods to the prediction of soaring weather. Due to the transportability of such computers numerical simulations can be carried out even on remote airfields. This paper deals with a simple convection model (briefly called Konpro) which was specially developed for the use on personal computers. It allows the simulation of the behaviour and strength of thermals and the development of cumulus clouds.

2. The General Forecasting Scheme

The Konpro model is embedded in a set of PC programs (in the following referred as *micromet*) which predict the vertical structure of the atmosphere during a day. The conception of *micromet* is shortly explained in this section before Konpro is described in detail.

Convective processes like thermals and cumulus convection depend on the temporal and spatial varying stratification of temperature and humidity, and on the diurnal energy input into the lower atmosphere. The latter is a function of season and daytime, and is additionally modified by meteorological parameters (large-scale screening, local fog, etc.), and by local factors like latitude, altitude, and land use.

The realization of the prognosis on a personal computer requires an economic treatment of these complex processes. This leads to a three-step process:

The vertical profiles of temperature and humidity are supposed to be changed during the day by

step 1: large-scale advection
step 2: diabatic heating
step 3: convective fluctuation

For a better understanding this scheme is also illustrated in figure 1.

The data base of the prognosis is given by several night or morning hour radiosoundings in the vicinity and in the upwind sector of the area for which a forecast is desired. This area will be called *target area* in the following.

Step 1 is carried out by two programs: the first one evaluates the measured profiles and interpolates temperature and humidity to levels of constant height. A second program then interpolates the values horizontally to the target area. The change of the profiles caused by horizontal advection is now estimated by this program. For this reason horizontal backward trajectories are constructed in different height levels, each starting in the target area. Vertical advection is not considered, however.

During step 2 diabatic heating is added to the advected profiles. The amount of heating is derived from the historic values given by Gold (1933), which are published in WMO (1978). The step 2 program calculates profiles for each hour between sunrise and sunset. An adiabatic lapse rate of temperature and a uniform specific humidity is assumed in the layer effected by heating.

Step 3 describes a single thermal event. This is done by the convection model Konpro, eventually. The model releases a test air bubble and looks for its behaviour where profiles calculated in step 1 and 2 are taken as a passive environment.

3. The Konpro Model

3.1 The model conception

Konpro is a so 1 called -½-*dimensional* model which is similar to the models introduced by Ogura and Takahashi (1971), Ossing (1979), and Nelson (1979). It solves prognostic equations for motion, temperature, mixing ratio of water vapor, and mixing ratio of cloud droplets within a vertical column which reaches from the ground to a suitable height of some thousand meters. This column represents the convective cell where thermal updraft and cumulus development can occur. The

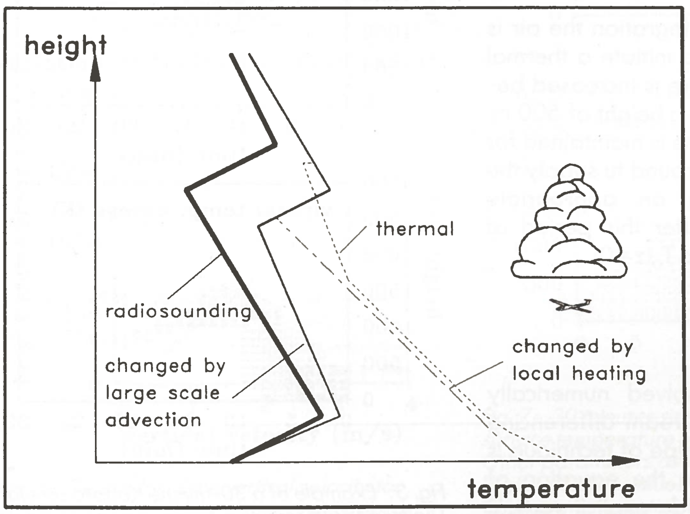

Fig. 1: Three-step change of a given morning hour sounding.

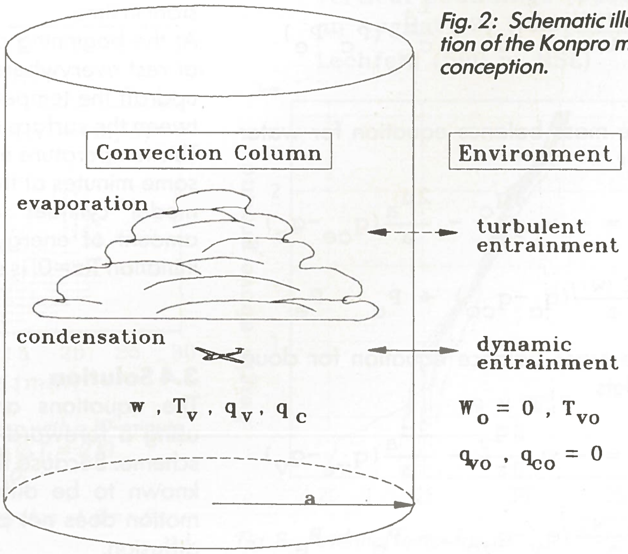

Fig. 2: Schematic illustration of the Konpro model conception.

ambient air outside this model cylinder is unchanged during the integration, but the model equations provide turbulent and dynamic *entrainment* of ambient air into the thermal column. This is meant by the "½ dimension". The dynamic entrainment or horizontal advection is calculated from the vertical divergence within the model cylinder. The turbulent entrainment or horizontal diffusion is governed by an entrainment coefficient and the horizontal wind shear. The latter is given by the strenght of the updraft and by the diameter of the convective cylinder. Konpro normally takes over the forecasted profiles of temperature and humidity for a certain daytime and keeps them as the ambient air condition. Outside the cylinder the air is assumed to be in hydrostatic equilibrium, and to have neither vertical velocity nor cloud droplets. See also figure 2.

3.2 Model equations

The five model variables w, u_a, T, q_v, and q_c are calculated from the following set of equations:

a) the equation of motion

$$\frac{\partial w}{\partial t} = - w\frac{\partial w}{\partial z} - \frac{2u_a}{a}(w_e - w)$$

$$+ g\frac{T_v - T_{vo}}{T_v} - \frac{2C|w|}{a}w$$

b) the continuity equation

$$u_a = -\frac{a}{\rho}\frac{\partial \rho w}{\partial z}$$

c) the thermodynamic equation

$$\frac{\partial T}{\partial t} = - w\left(\frac{\partial T}{\partial z} + \gamma_d\right) - \frac{2u_a}{a}(T_e - T)$$

$$- \frac{2C|w|}{a}(T - T_o) + \frac{l_d}{c_p}(P_c - P_e)$$

d) the mass balance equation for water vapor

$$\frac{\partial q_c}{\partial t} = - w\frac{\partial q_c}{\partial z} - \frac{2u_a}{a}(q_{ce} - q_c)$$

$$- \frac{2C|w|}{a}(q_c - q_{co}) + P_c - P_e$$

e) the mass balance equation for cloud droplets

$$\frac{\partial q_v}{\partial t} = - w\frac{\partial q_v}{\partial z} - \frac{2u_a}{a}(q_{ve} - q_v)$$

$$- \frac{2C|w|}{a}(q_v - q_{vo}) - P_c + P_e$$

T_v is the virtual temperature. T_o, T_{vo}, and q_{vo} belong to the profile of the ambient air.

The terms of dynamic entrainment use

$$w_e = \begin{cases} 0 \\ w \end{cases} ; \quad T_e = \begin{cases} T_o \\ T \end{cases} ; \quad q_{ve} = \begin{cases} q_{vo} \\ q_v \end{cases} ; \quad q_{ce} = \begin{cases} q_{co} & \text{for } u_a < 0 \\ q_c & \text{for } u_a \geq 0 \end{cases}$$

Condensation is assumed immediately after oversaturation occurs. Therefore the condensation rate P_c is calculated as

$$P_c = \frac{q_v - q_{vs}}{\Delta t}$$

q_{vs} is the saturation mixing ratio and Δt is the time step. The evaporation rate is determined by

$$P_e = \frac{1}{\rho}\,\frac{(q_v/q_{vs} - 1)\,(10^{-3}\,\rho\, q_c)^{0.525}}{700 + (0.41 \cdot 10^6 / p_{vs})}$$

(variables in SI-units)

following Ogura and Takahashi.

3.3 Boundary condition and initialization

The set of equations is solved using the following boundary conditions:

at z=0 (bottom): $w = 0$, $T = T_o(z=0) + \Delta T_i$, $q_v = q_{vo}(z=0)$, $q_c = 0$

at z=H (top): following OGURA and TAKAHASHI.

The lateral boundaries are given by the profiles of the ambient air which are constant in time.

At the beginning of integration the air is at rest everywhere. To initiate a thermal updraft the temperature is increased between the surface and a height of 500 m. This temperature excess is maintained for some minutes at the ground tu supply the model cylinder with an appropriate amount of energy. After this period of initiation T(z=0) is set to T_o(z=0).

3.4 Solution

The equations are solved numerically using a foreward-upstream differencing scheme. Because this type of technique is known to be diffusive the equation of motion does not provide explicit vertical diffusion.

Throughout the simulations in this paper the following conditions were taken:

- height of the model: H = 4000 m
- vertical grid spacing: Δz = 100 m
- time step: Δt = 10 s

The result of a typical model run is represented in figure 3. The time-height diagrams show three stages of the thermal life cycle. During the first 10 minutes the updraft develops, gains height, and finally penetrates into the stable layer above 1100 m AGL (above ground level). Between 10 and 20 minutes of integration the thermal is in its mature stage where the liquid water content indicates the existence of a cumulus cloud. During the last 10 minutes the thermal decays. The

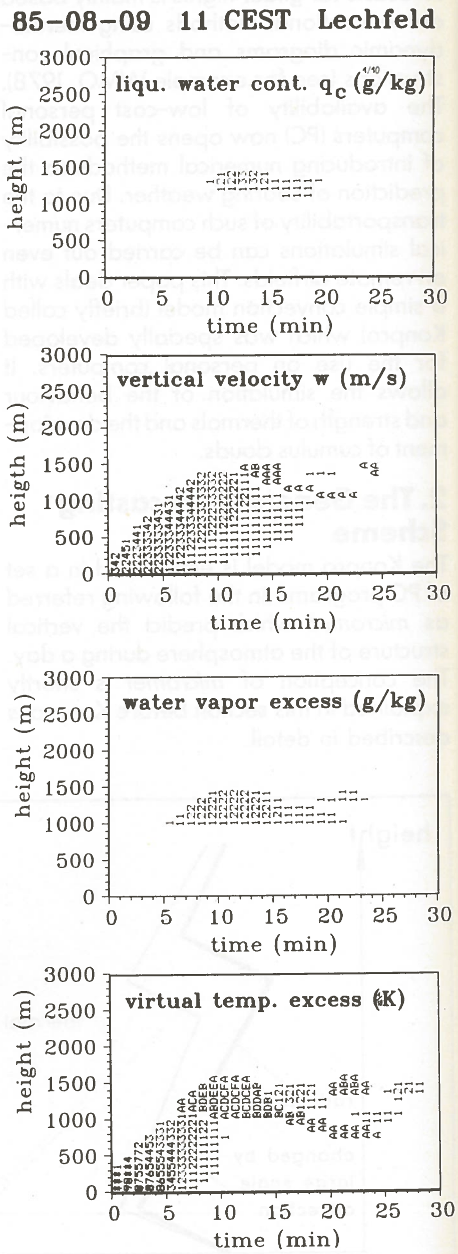

Fig. 3: Example of a 30-minute Konpro simulation Digits: positive values. Characters: negative values (A≡ −1, B≡ −2, etc.)

temperature and humidity differences between the convective cell and its environment become very small, and the vertical velocity vanishes.

4. Sensitivity

Some model parameters cannot be taken from measurements, but have to be prescribed. These are

- the turbulent entrainment coefficient C
- the radius of the convective column a
- the duration and intensity of surface temperature excess ΔT_i

In a first test the entrainment coefficient C was varied between 0.1 and 0.001. The entrainment acts like friction. Thus, a high value of C reduces the vertical velocity. The temperature and humidity differences between the convective column and its environment also decrease due to more effective entrainment, which diminishes the buoyancy and also retards the updraft.
Figure 4 shows the vertical profiles of w after 10 minutes of integration for three values of C. Between C = 0.01 and C = 0.001 the vertical velocity changes by less than 5%.

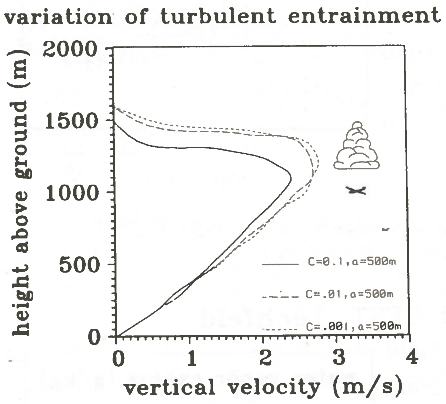

Fig. 4: Sensitivity of the vertical velocity to variations of the entrainment parameter C.

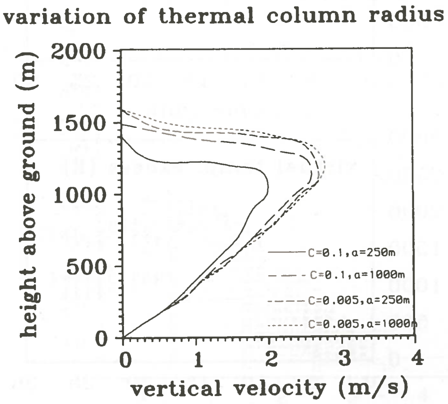

Fig. 5: Sensitivity of the vertical velocity to variations of the radius of the convective column.

A second test was carried out with different values of the cylinder radius a. Smaller values of a correspond with more entrainment. This tends to decrease the vertical motion. Figure 5 shows that the maximum updraft speed decreases by 30% if a is reduced from 1000 m to 250 m while C = 0.1. For small values of C the effect is less pronounced. During the following simulations the entrainment parameter was taken as C = 0.005. This value is also recommended by OGURA and TAKAHASHI. The radius of the convective column was chosen to a = 500 m. This seems to be a reasonable quantity for shallow cumulus convection.

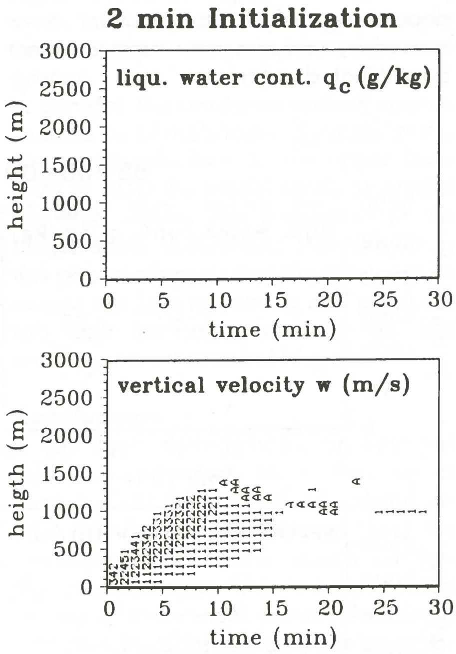

Fig. 6: 30 minutes simulation with a 2-minute surface temperature excess (ΔT_i = 2 K)
Digits: positive values
Characters: negative values

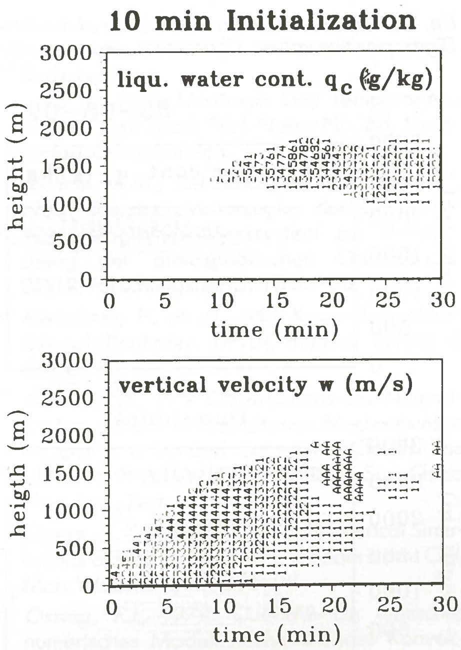

Fig. 7: 30 minutes simulation with a 10-minute surface temperature excess (ΔT_i = 2 K)
Other parameters as in fig. 6.
Digits: positive values
Characters: negative values (A≡ −1, B≡ −2, etc.)

In a third test the duration of increased surface temperature (ΔT_i = 2 K) was varied from 2 to 10 minutes. The sensitivity to this change is very significant (figure 6 and 7). While the updraft reaches a height of only 1300 m after two minutes temperature excess near the ground, it extends up to 1700 m in the case of 10 minutes. Moreover, two minutes of increased ground level temperature do not even bring about a cumulus cloud which has developed in the other case.

5. Comparison with measurements

In this section Konpro results are compared with measurements. Appropriate data were gained during the Koop campaign (see Meischner et. al., 1981 or Jochum, Reinhardt, Willeke, 1984) which was accomplished by the German Aerospace Research Establishment (DFVLR) in summer 1983. Between 11 and 14 CEST (Central European Summer Time) three motor gliders measured temperature and humidity fluctuations in different levels along a 12-km flight track over flat terrain 60 km west of Munich. At the same time vertical soundings were recorded by a fourth aircraft. Simulations will be shown for August 9th, 1983, which has been an undisturbed summer day.
Figures 8 and 9 show the measured profiles of potential temperature and specific humidity between 9 and 14 CEST. One

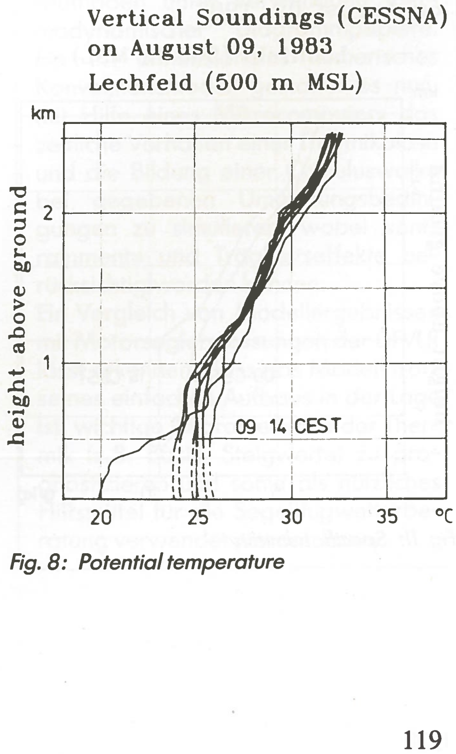

Fig. 8: Potential temperature

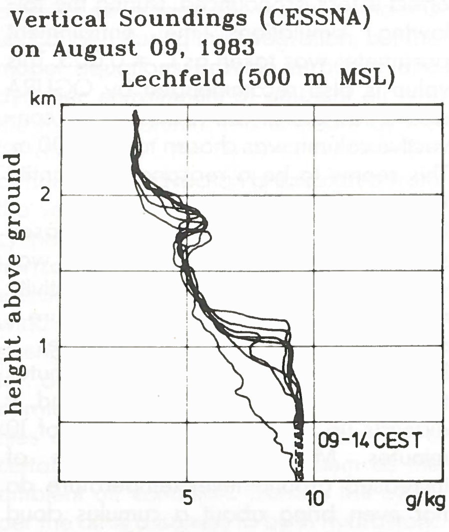

Fig. 9: Specific humidity

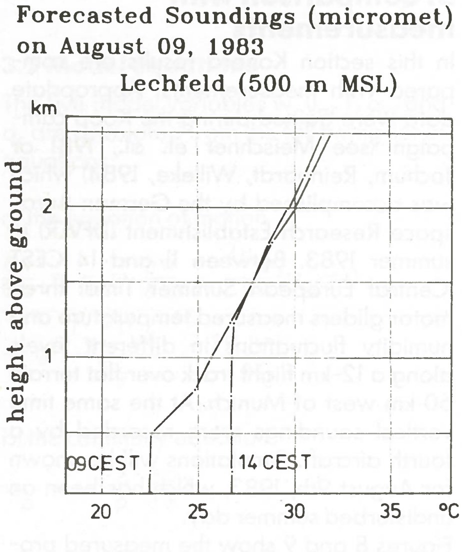

Fig. 10: Potential temperature

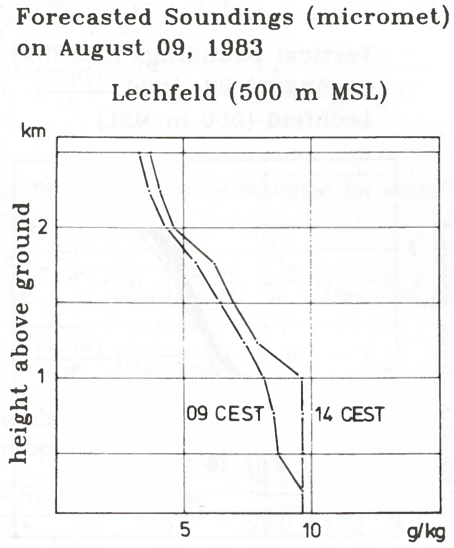

Fig. 11: Specific humidity

can clearly see the development of a well-mixed layer which extends up to 1200 m above ground level at 14 CEST. The micromet prognosis for 9 and 14 CEST is illustrated in figure 10 and 11. The thickness of the convective layer is in good agreement with the measurements. On the other hand absolute values deviate from the soundings in some layers. This is probably a consequence of the height dependency of a measurement error caused by compression which could not be eliminated so far.

Figures 12 and 13 show the results of 30 minutes of integration with a = 500 m, C = 0.005, and 5 minutes of $\Delta T_i = 2$ K surface temperature excess. The micromet forecasts for 12 and 14 CEST were taken as ambient air profiles. A cloud forms after 10 minutes in either case. The cloud base establishes in 1200 m at 12 CEST, and in 1500 m at 14 CEST. The tops reach heights of 1600 m (12 CEST) and 2200 m (14 CEST). This coincides quite well with visual observations from the aircraft. The reported cloud cover was 1-2/8 of cumulus.

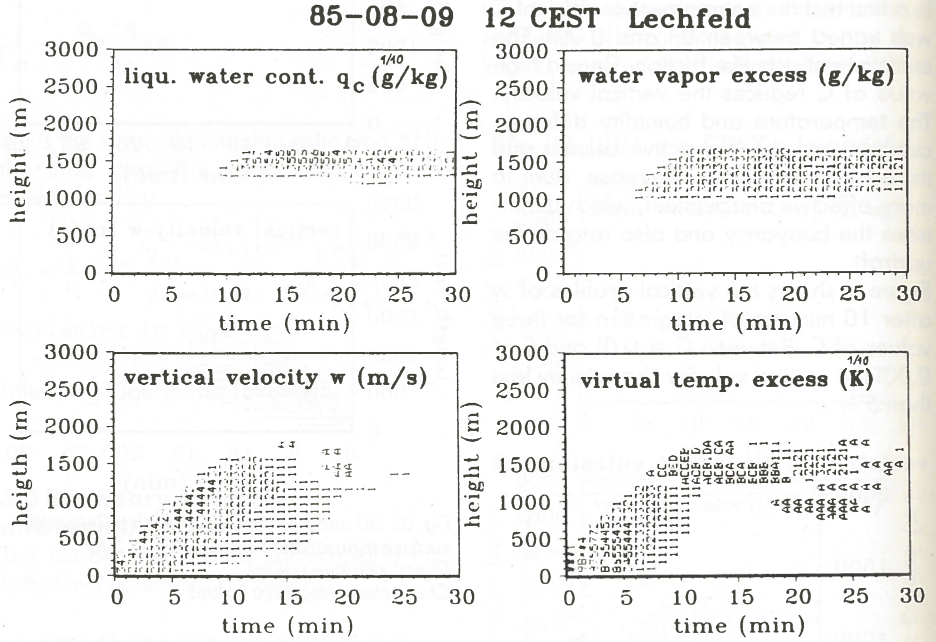

Fig. 12: Model simulation on the base of the forecasted profiles for Aug. 9, 1983, 12 CEST
Digits: positive values. Characters: negative values (A≡ −1, B≡ −2, etc.)

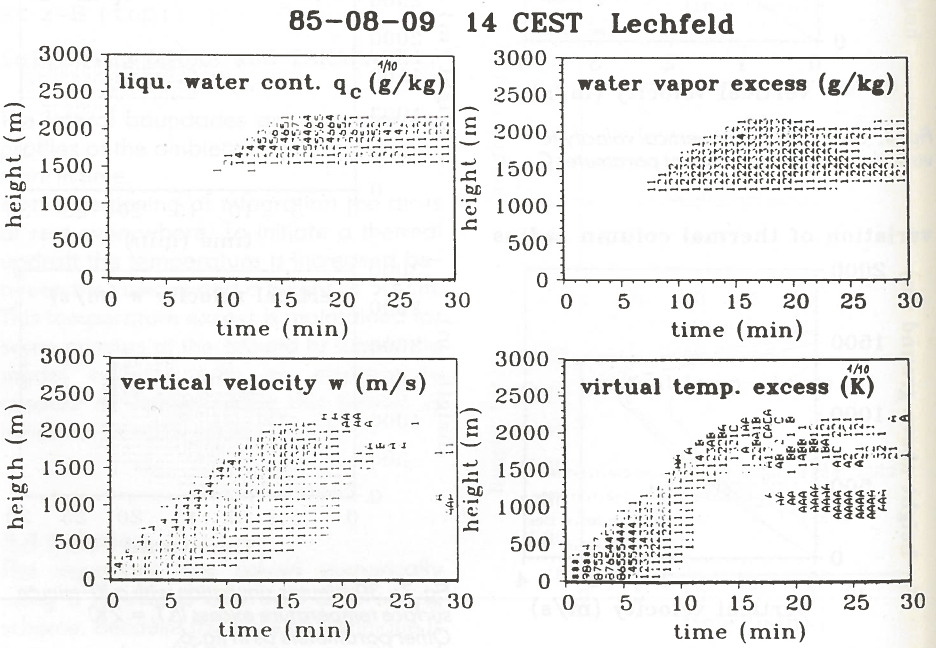

Fig. 13: Model simulation on the base of the forecasted profiles for Aug. 9, 1983, 14 CEST
Digits: positive values. Characters: negative values (A≡ −1, B≡ −2, etc.)

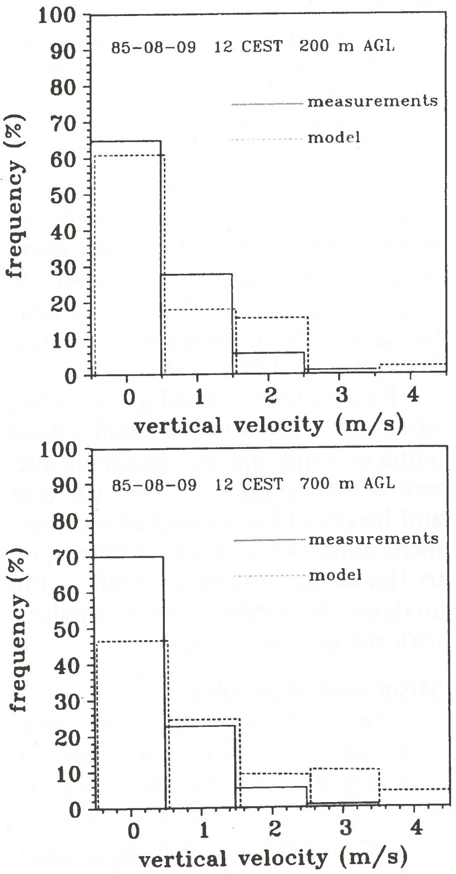

Fig. 14: Calculated and measured frequency distribution of the vertical velocity (12 CEST).

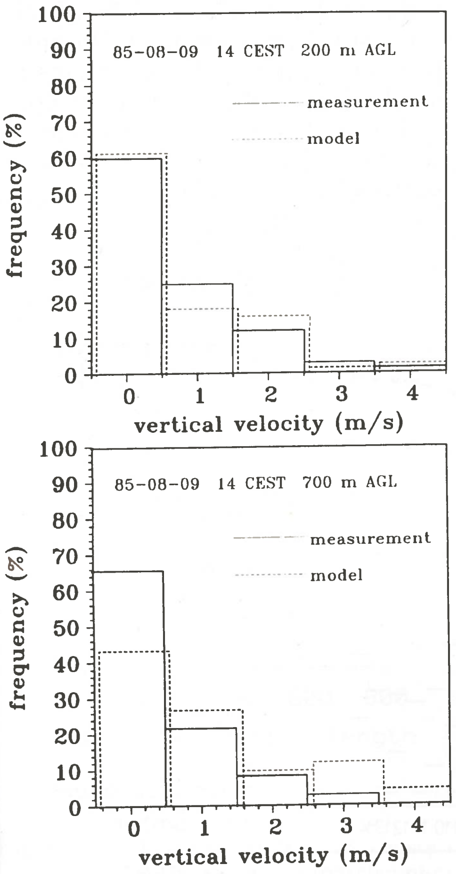

Fig. 15: Calculated and measured frequency distribution of the vertical velocity (14 CEST).

The frequency distributions of vertical velocities are given in figure 14 and 15. Since the model can predict vertical motion only within the convective column the evaluation of measurements was restricted to positive values of w. Nevertheless one has to keep in mind that the frequency distributions of the measurements were derived from samples taken along a 12-km flight track, while the distributions of the simulated values were gained from 180 time steps during the 30 minutes integration.

In general, the simulated updraft speeds seem to be of the same magnitude as the measured velocities. In the upper level (700 m AGL) the model tends to predict too high values. The evaluation of the temperature fluctuations (not shown in this paper) suggests that the temperature excess is a little too strong and produces too high vertical speeds in the first minutes of the thermal's life cycle.

Conclusions

It has been shown that even low-cost personal computers allow the use of numerical models to predict the stratification, the strength of thermals, and the development of cumulus clouds. But further measurements have to be evaluated to adjust free model parameters. Once validated the Konpro model can be a useful tool for weather prediction on glider airfields. The model can substitute graphical methods without too much additional effort, and it provides the consideration of entrainment and inertia effects.

References

Gold, E., 1933: Maximum Day Temperatures and the Tephigram Prof. Notes No. 63, Meteorolog. Office London.

Jochum, A.M., Reinhardt, M.E., Willeke, H., 1984: Die drei Motorsegler der DFVLR–ein meteorologisches Messsystem zur Untersuchung der atmosphärischen Grenzschicht. DFVLR-Forschungsbericht FB 84-50.

Meischner, P., et. al., 1981: Koop–Konvektion Oberpfaffenhofen. DFVLR, Interner Bericht IB 553 81/8.

Nelson, L.D., 1979: Observations and Numerical Simulations of Precipitation Mechanisms in Natural and Seeded Convective Clouds. The Univ. of Chicago, Dept. Geoph. Sc., Cloud Phys. Lab., Technical Note 54.

Ogura, Y., Takahashi, T., 1971: Numerical Simulations of the Life Cycle of a Thunderstorm Cell. Mon. Wea. Rev., 99, 895–911

Ossing, F.J., 1979: CUNIMB–Ein einfaches numerisches Modell hochreichender Konvektion. Diplomarbeit, Inst. Geophys. Wiss., FU Berlin.

World Meteorological Organization (WMO), 1978: Handbook of Meteorological Forecasting for Soaring Flights. Prepared by OSTIV, Technical Note 158.

List of symbols

- a radius of the convective cylinder
- C turbulent entrainment parameter
- c_p specific heat capacity
- Δt time step
- Δz vertical grid spacing
- l_v specific condensation heat
- p_{vs} saturation vapor pressure
- P_c condensation rate
- P_e evaporation rate
- q_c mixing ratio of cloud droplets
- q_v mixing ratio of water vapor
- ϱ density of air
- t time
- T temperature
- T_v virtual temperature $T_v = T(1+0.608\,q_v)$
- u_a horizontal advection speed
- w vertical velocity

Summary

A simple numerical model of cumulus convection is introduced which can be run even on a personal computer. In addition to conventional methods the model also incorporates the effects of entrainment and inertia. After some sensibility tests model results are verified with data of thermal turbulence taken from aircraft measurements. The model seems to predict the vertical velocity and the height of cumulus clouds fairly well.

Zusammenfassung

Die Konvektionsprognose für Segelflugwettervorhersagen basiert bis heute weitgehend auf graphischen Methoden unter Verwendung thermodynamischer Diagrammpapiere. Ein 1½ dimensionales numerisches Konvektionsmodell gestattet es nun, mit Hilfe eines Mikrocomputers das zeitliche Verhalten einer Thermikblase und die Bildung einer Cumuluswolke bei gegebenen Umgebungsbedingungen zu simulieren, wobei «entrainment» und Trägheitseffekte berücksichtigtwerden können.

Ein Vergleich von Modellergebnissen mit Motorseglermessungen der DFVLR lässt erkennen, dass das Modell trotz seines einfachen Aufbaus in der Lage ist, wichtige Charakteristika der Thermik (z.B. Basis, Steigwerte) zu prognostizieren und somit als nützliches Hilfsmittel für die Segelflugwetterberatung verwendet werden kann.